ATLANTIS PRESS

*Advances in Engineering Research, volume 141*

5th International Conference on Mechatronics, Materials, Chemistry and Computer Engineering (ICMMCCE 2017)

# Identifying the number of $WS_2$ layers via Raman and photoluminescence spectrum

**Shuai Qiao[1,a] , Hang Yang[1,b], Zongqi Bai[2,c], Gang Peng[1,d] and Xueao Zhang[1,e*]**

[1]College of Science, National University of Defense Technology, Changsha 410073, China

[2]Department of Physics and Astronomy, Shanghai Jiaotong University, Shanghai 200240, China

[a]qiaoshuai62@163.com, [b]yanghangNUDT@163.com,

[c]545154780@sjtu.edu.cn, [d]penggang@nudt.edu.cn,

[e]xazhang@nudt.edu.cn

*Corresponding author

**Keywords:** $WS_2$, Number of layers, Raman, Photoluminescence

**Abstract:** Recently**,** two-dimensional atomic layers of transition metal dichalcogenides (TMDs) have drawn more attention because of their remarkable electronic and optical properties. How to effectively identify the number of TMDs layers becomes an important issue. Here, we report the determination of the number of tungsten disulfide ($WS_2$) layers using Raman scattering and photoluminescence (PL) spectrum. Under the excitation of 532 nm laser, the Raman scattering of $WS_2$ shows rich spectrum information. With the number of layers increase, the peak of $E^1_{2g}(\Gamma)$ phonon mode of $WS_2$ redshifts while the peak of $A_{1g}(\Gamma)$ blue shifts. For PL measurements, monolayer $WS_2$ exhibits a performance of direct-bandgap. As the number of layers change from three to single, the PL peak intensity of $WS_2$ increases, and the peak shifts to the short wavelength. Raman and PL mapping show coincident results. Our study establishes a systematical, noninvasive fingerprint path to identify different layers $WS_2$ using Raman and PL spectrum simultaneously.

## Introduction.

Two-dimensional (2D) transition metal dichalcogenides (TMDs) have been well-known because of their sizable bandgap[1,2], strong photoluminescence (PL)[3-5], and promising applications in optoelectronics[6,7] etc. As a typical example of the TMDs family, $WS_2$ thin layers are less studied compared with other TMDs. Actually, $WS_2$ not only possesses same advantages but also possesses some particular advantages compared to other 2D TMDs materials. For example, $WS_2$ exhibits strong thermal stability[8] and ambipolar field-modulation behavior[9].A calculation also shows that comparing with other 2D crystals, within the ballistic regime the monolayer $WS_2$ transistors have the best performance[10]. Moreover, $WS_2$ exhibits nearly three times larger valence band splitting compared to $MoS_2$[11], which allows easier observation of the valley hall effect, has also been achieved. $WS_2$ also has a wider operation temperature range as lubricants[12]. Both Raman spectrum and photoluminescence(PL) measurements have become a powerful and noninvasive tools for studying semiconducting TMDs[13-15], Studying the Raman and PL spectrum is still deserved. Raman spectrum and PL measurements can not only be used to identify the number of layers, but also can probe strain and doping/defects etc. Raman can rapidly identify the layers of graphene and other 2D materials[16-18], as for TMDs, the Raman spectrum is more complicated and richer because of a monolayer of these TMDs is composed of not one but three atoms[19,20]. There are the paper introduce identification of layers of $WS_2$ using Raman spectrum[21], also there have been the synthesis of single-layer $WS_2$ triangular islands and observed room-temperature photoluminescence (PL) with the layers of $WS_2$[22]. But there is no one studies different layers $WS_2$ using Raman and PL spectrum simultaneously.

In this paper, we provide comprehensive study of $WS_2$ with the Raman and PL as a function of the number of layers. Obviously, PL is much more sensitive to the layer of the $WS_2$ than Raman

scattering and can thus be more reliably used to determine the layers in semiconducting TMDs, however, the Raman scattering is more rich，it can also probe subtle details in the electronic band structure and phonon dispersion[16,23].This paper also provides Raman and PL mapping of the $WS_2$ sample.

**Experimental Details.**

The sample of $WS_2$ nanoflakes was obtained from the commercially available $WS_2$ crystals onto 300 nm $SiO_2$/Si substrates using mechanical exfoliation technique[24]. Then, it was necessary to search suitable sample under the optical microscope. We can judge few-layer even single-layer of $WS_2$ with its optical characteristic. There is no denying using Raman and PL spectrum to characterize $WS_2$ nanoflakes is more exact. Confocal Raman Microscopy is a unique tool that enables non-destructive imaging of the sample. Here, we apply WITec Alpha 300R confocal microscope-based Raman spectrometer to characterize the $WS_2$ nanoflakes. WITec Alpha300R is an advanced Confocal Raman Microscope that integrates a high-transmission Raman spectroscopy system and a highly sensitive confocal microscope. It can achieve single point Raman and PL spectrum acquisition. The equipment also have automated confocal Raman imaging, that can achieve Raman spectral imaging, acquisition of a complete Raman spectra at every image pixel. In the experiment 532 nm laser excitation was applied, and the laser was kept same power at all time.

**Results and Discussion.**

Figure 1 shows the atomic structure of the $WS_2$ crystal. $WS_2$ crystal organized in a trigonal prismatic arrangement of S-W-S atoms. Every single plane of $WS_2$ contains a trilayer compose of an individual tungsten layer, sandwiched between two sulfur layers in a trigonal prismatic coordination, as shown in Figure 1(a).

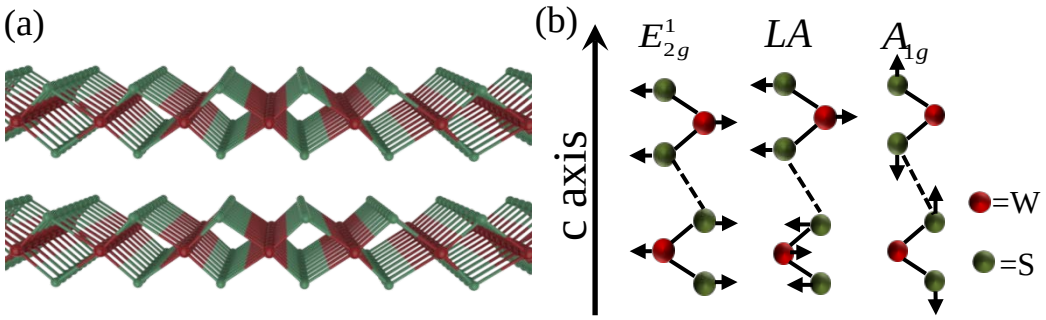


Figure 1 (a) Primitive cell and three-dimensional schematic representation of a typical $WS_2$ structure with the sulfur atoms in red and the tungsten atoms in blue. (b) Schematic diagram of the first-order Raman active modes of $WS_2$.

Figure 1(b) is the schematic diagram of the first-order Raman active modes of $WS_2$ nanoflakes, which show $E^1_{2g}(\Gamma)$, $A_{1g}(\Gamma)$ and LA(M). Among them $E^1_{2g}(\Gamma)$ and $A_{1g}(\Gamma)$ are the two optical phonon modes at the Brillouin zone center. $E^1_{2g}(\Gamma)$ correspond to an in-plane optical mode, another $A_{1g}(\Gamma)$ is to out-of-plane vibrations of the sulfur atoms. LA(M) is the one longitudinal acoustic mode at the M point, which is in-plane collective movements of the atoms in the lattice, similar to the sound waves. The dashed line represents the weak inter-layer van der waals interaction. Additional peaks correspond to the multi-phonon modes which are combined with these first-order modes [23,24].

Raman spectrum of the $WS_2$ nanoflakes was performed with the 532 nm laser excitations. Figure 2 shows the Raman spectrum change with the number of $WS_2$ layers. The Raman spectrum displays many first-order, second-order and other combination peaks. There we only mark obvious peaks, the first-order modes, LA(M) at about 174 $cm^{-1}$, $E^1_{2g}(\Gamma)$ at about 357 $cm^{-1}$ and $A_{1g}(\Gamma)$ at about 420 $cm^{-1}$. Due to the $E^1_{2g}(\Gamma)$ and $A_{1g}(\Gamma)$ exist obvious variation of the number of layers, we focused on the variety of those two peaks.

From the Raman spectrum, it is obvious that an increase appear in the absolute intensity with increasing number of layers from 1L to 3L. However, the intensities of bulk are lower than of the 1L instance and is mainly attributed to optical interference in both the excitation laser and the Raman signal emitted by the sample [21].Such behavior have been observed in graphene [25] and $MoS_2$ [19] deposited on $SiO_2$/Si substrates before.

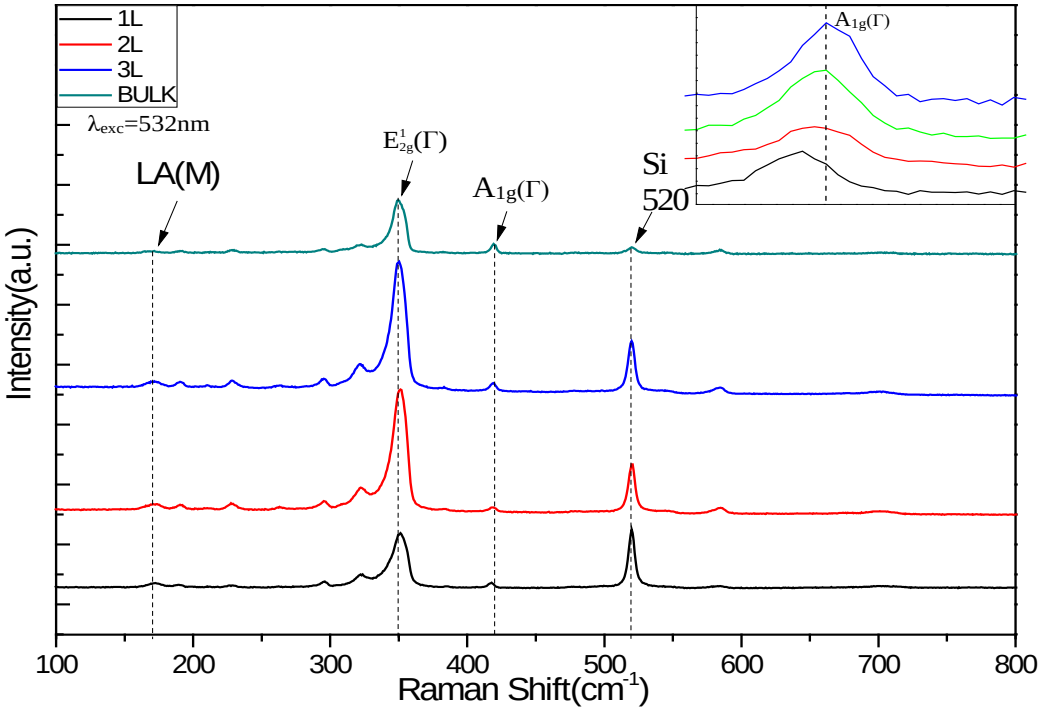


Figure 2 Room-temperature Raman spectrum of different layers $WS_2$, using the 532nm laser excitation. The inset shows the detail of $A_{1g}(\Gamma)$ peak.

It also can be seen as increasing the number of layers, the $A_{1g}(\Gamma)$ mode exhibits blue-shifts. The $E^1_{2g}(\Gamma)$ phonon modes, on the contrary, exhibits redshifts. So the wave number difference between $A_{1g}(\Gamma)$ mode and $E^1_{2g}(\Gamma)$ modes are increases with the number of $WS_2$ layers increasing. Table1 summarizes the peaks position of the $A_{1g}(\Gamma)$ and $E^1_{2g}(\Gamma)$ Raman modes as a function of the number of layers.

Table 1 The frequency of the $A_{1g}(\Gamma)$ and $E^1_{2g}(\Gamma)$, as a function of the number of layers, using the 532 nm laser excitation.

| | 1-layer | 2-layers | 3-layers | Bulk |
|---|---|---|---|---|
| $E^1_{2g}(\Gamma)$( $cm^{-1}$) | 352.1 | 350.9 | 349.8 | 348.7 |
| $A_{1g}(\Gamma)$($cm^{-1}$) | 417.5 | 418.3 | 418.7 | 419.1 |

Finally, it is clear that the absolute intensity of 520nm Si peak significantly decrease with increasing number of layers. The reason is with the increasing number of layers the Raman laser that arrived Si surface is gradually weak, so the Raman scattering intensity becomes weak.

It should be noticed that there is a second-order Raman peak 2LA(M) in resonance overlapped the $E^1_{2g}(\Gamma)$ peak. It can separate the two peaks by the multi-peak Lorentzian fitting. And it is remarkable that the 2LA(M) mode is close to twice the intensity of the first-order $A_{1g}(\Gamma)$ due to a double resonance process[21].

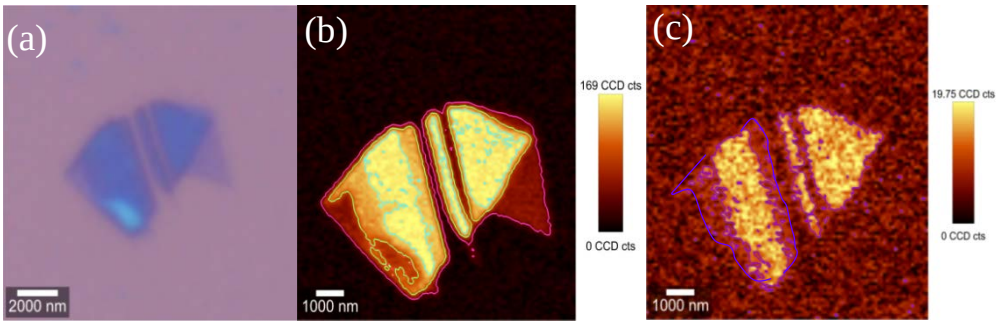


Figure 3 (a) Optical image of $WS_2$ sample. (b) and (c) Raman mappings of the $WS_2$ sample: (b) Intensity of the $E^1_{2g}(\Gamma)$ mode, (c) Intensity of the $A_{1g}(\Gamma)$ mode(using 532 nm laser excitation)

Figure 3(a) is the optical image of the sample. The layer of $WS_2$ sample can be approximately judged. Raman mapping of the sample at $\lambda_{exc}$=532 nm provides spatial maps of the $E^1_{2g}(\Gamma)$ intensity and the $A_{1g}(\Gamma)$ mode intensity, as shown in Figure 3(b), (c). The absolute intensity of the $E^1_{2g}(\Gamma)$ and $A_{1g}(\Gamma)$ mode increases with decreasing the number of layers, similar to above result of Raman spectrum and consistent with the optical image.

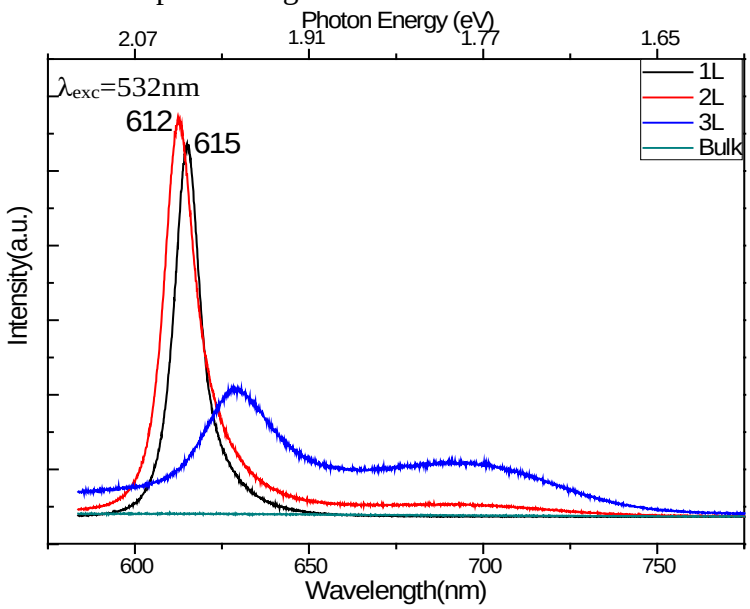


Figure 4 Room-temperature PL spectrum of different layers $WS_2$, using the 532 nm laser excitation.

Furthermore, Raman mapping shows lower left corner layers is fewer than middle $WS_2$ of the sample. The result is opposite with the optical image. It may be because the residue of tape affects the optical properties of $WS_2$ sample. It reveals the accuracy of Raman characterization.

Bulk $WS_2$ is an indirect-bandgap(1.4eV) semiconductor, however, when exfoliated into single-layer, $WS_2$ transit to a direct-bandgap(2.1eV) material[26]. Figure 4 shows the room-temperature PL spectrum of different layers $WS_2$, using the 532 nm laser excitation.

For 1L and 2L $WS_2$, the PL peaks locate around 615 nm and 612 nm. According to the equation $Eg=hc/e\lambda$, it can be obtained the band gaps are about 2.02 eV and 2.03 eV separately. For the 3L $WS_2$, the PL peak shifts to the long wavelength and the absolute intensity is obvious lower than 1L and 2L, indicating that the 2L band gap have not completely evolve to the indirect-bandgap. In contrast, the PL peak for 3L suggests its direct band gap nearly almost not present. Furthermore, there is no any PL peak of bulk $WS_2$, which gives a clear evidence of above transition. As reported in a previous work [10], $WS_2$ performed a transition from indirect-gap of bulk to direct-gap of few-layer.

Figure 5 show the mapping of the PL peak spectrum position. It is in correspondence with the above PL spectrum results. Meanwhile, it shows that lower left corner layers are fewer than middle $WS_2$ of the sample once again.

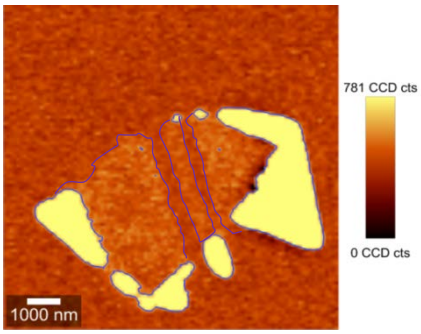


Figure 5 Corresponding Mappings of the PL peak spectrum position (absolute maximum intensity of the PL peak) about the $WS_2$ sample (using 532 nm laser excitation)

**Conclusions.**

In this study, different layers of $WS_2$ Raman and photoluminescence behavior were systematically investigated using 532nm laser. For the Raman scattering, by studying three different layers of $WS_2$, it is obvious that an increase emerges in the absolute intensity with increasing number of layers from 1L to 3L. With the increase of the number of layers, the peak of $E^1_{2g}(\Gamma)$ phonon mode of $WS_2$ red-shifts while the peak of $A_{1g}(\Gamma)$ blue-shifts. As for PL, bulk $WS_2$ exhibited an indirect-bandgap characteristic. Other few-layers exhibited a direct-bandgap especially for single-layer. The Raman and PL mapping also were investigated and the result was same with single Raman and PL spectrum. Both Raman frequency shifts and PL intensity can give an identification layer of $WS_2$.

**Acknowledgements.**

The authors acknowledge financial support from the National Natural Science Foundation of China(No.11574395), the National Natural Science Foundation of China (No.61675234), the Open Research Fund Program of the State Key Laboratory of Low-Dimensional Quantum Physics (No.KF201411), the Advanced Research Foundation of the National University of Defense Technology (No.zk16-03-40), the Open Foundation of State Key Laboratory of High Performance Computing (No.201301-02) and the research project of National University of Defense Technology (No.JC15-02-01).

**References.**

1.Mak, K. F., Lee, C., Hone, J., Shan, J., Heinz, T. F. (2010) Atomically Thin $MoS_2$: A New Direct-Gap Semiconductor. Phys. Rev. Lett., 105, 136805.

2. Yoffe, A. D. (1993) Layer compounds. Annu. Rev. Mater. Sci., 3, 147.

3. Splendiani A., Sun L., Zhang Y., Li T., Kim J., Chim C.Y., Galli G., Wang F. (2010) Emerging Photoluminescence in Monolayer $MoS_2$. Nano Lett. 10, 1271.

4.Eda, G., Yamaguchi, H., Voiry, D., Fujita, T., Chen, M., Chhowalla, M. (2011) Photoluminescence from Chemically Exfoliated $MoS_2$. Nano Lett., 11, 5111.

5. Zhao, W., Ghorannevis, Z., Chu, L., Toh, M., Kloc, C., Tan,P.-H., Eda, G. (2012) Evolution of Electronic Structure in Atomically Thin Sheets of $WS_2$ and $WSe_2$. ACS Nano., 7, 791.

6. H. L. Zeng, J. F. Dai, W. Yao, D. Xiao, and X. D. Cui, (2012) Valley polarization in $MoS_2$ monolayers by optical pumping. Nat. Nanotechnol., 7, 490.

7. Y. J. Zhang, T. Oka, R. Suzuki, J. T. Ye, and Y. Iwasa, (2014) Electrically switchable chiral lighe-emitting transistor. Science, 344, 725.

8. Brainard, W. A. (1969) The Thermal Stability And Friction Of The Disulfides, Diselenides, And Ditellurides Of Molybdenum And Tungsten In Vacuum ($10^{-9}$ to $10^{-6}$ torr). NASA, Washington.

9. W. Sik Hwang, M. Remskar, R. Yan, V. Protasenko, et al. (2012) Transistors with chemically synthesized layered semiconductor $WS_2$ exhibiting $10^5$ room temperature modulation and ambipolar behavior. Appl. Phys. Lett., 101, 418.

10. Leitao, L., Kumar, S. B., Yijian, O. Jing, G. (2011) Performance Limits of Monolayer Transition Metal Dichalcogenide Transistors. IEEE Transactions on Electron Devices, 58, 3042.

11. Zhu Z.Y., Cheng Y.C., Schwingenschlögl U., (2011) Grüneisen parameter of the G mode of strained monolayer graphene. Phys. Rev. B, 83, 115449.

12. Prasad, S. V., McDevitt, N. T. & Zabinski, J. S. (2000) Tribology of tungsten disulfide nanocrystalline zinc oxide adaptive lubricant films from ambient to 500℃. Wear, 237, 186.

13. Najmaei, S., Liu, Z., Ajayan, P. M. & Lou, J. (2012) Thermal effects on the characteristic Raman spectrum of molybdenum disulfide ($MoS_2$) of varying thicknesses. Appl. Phys. Lett., 100, 1271.

14. Zhan, Y., Liu, Z., Najmaei, S., Ajayan, P. M. & J, L. (2012) Large-Area Vapor-Phase Growth and Characterization of $MoS_2$ Atomic Layers on a $SiO_2$ Substrate. Small, 8, 966.

15. Lee, Y. H. et al. (2012) Synthesis of large-area $MoS_2$ atomic layers with Chemical Vapor Deposition. Advanced Materials, 24, 2320.

16. Ferrari, A.C.et al. (2006) Raman spectrum of graphene and graphene layers. Phys. Rev. Lett. 97.

17. Gupta, A., Chen, G., Joshi, P., Tadigadapa, S. & Eklund, P. C. (2006) Raman scattering from high-frequency phonons in supported n-graphene layer films. Nano Lett. 6, 2667.

18. Gorbachev, R. V. et al. (2011) Hunting for Monolayer Boron Nitride: Optical and Raman Signatures. Small 7, 465.

19. Lee, C. et al. (2010) Anomalous Lattice Vibrations of Single- and Few-Layer $MoS_2$. Acs Nano 4, 2695.

20. Molina-Sanchez, A. & Wirtz, L. (2011) Phonons in single-layer and few-layer $MoS_2$ and $WS_2$. Phys. Rev. B 84, 155413.

21. Ayse Berkdemir, Humberto R. Gutierrez, Andres R.Botello-Mendez, et al. (2013) Identification of individual and few layers of $WS_2$ using Raman Spectroscopy. Scientific Reports, 3,1755.

22. Humberto R.Gutierrez, Nestor Perea-Lopez, Ana Laura Elías, et al. (2012) Extraordinary Room-Temperature Photoluminescence in Triangular $WS_2$ Monolayers. nano lett., 13,3447.

23. Frey G., Tenne R., Matthews M. J., Dresselhaus M. S., Dresselhaus G. (1998) Optical properties of $MS_2$ (M=Mo,W) inorganic fullerene-like and nanotube material optical absorption and resonance Raman measurements. Journal of Materials Research. 13, 2412.

24. Stacy A.M., Hodul D.T. (1985) Raman spectra of IVB and VIB transition metal disulfides using laser energies near the absorption edges. Journal of Physics & Chemistry of Solids, 46, 405.

25. Wang Y.Y., Ni Z.H., Shen Z.X., Wang H.M., Wu Y.H. (2008) Interference enhancement of Raman signal of graphene. Appl. Phys. Lett., 92, 666.

26. Kuc A., Zibouche N., Heine T. (2011) Influence of quantum confinement on the electronic structure of the transition metal sulfide $TS_2$. Phys. Rev. B, 83, 2237.